International Journal of Bifurcation and Chaos, Vol. 23, No. 6 (2013) 1330021 (21 pages)

DOI: 10.1142/S0218127413300218

ON THE DYNAMICS OF A SIMPLE RATIONAL PLANAR MAP

CHRISTOFOROS SOMARAKIS*
Department of Applied Mathematics,
University of Maryland, College Park, USA
csomarak@umd.edu

JOHN S. BARAS*
Department of Electrical and Computer Engineering,
University of Maryland, College Park, USA
baras@umd.edu

Received August 12, 2012; Revised November 1, 2012

The dynamics of the map

$$F\begin{pmatrix} x \\ y \end{pmatrix} = \begin{pmatrix} -\dfrac{ax}{1+y^2} \\ x + by \end{pmatrix}$$

are discussed for various values of its parameters. Despite the simple algebraic structure, this map, recently introduced in the literature, is very rich in nonlinear phenomena. Multiple strange attractors, transitions to chaos via period-doubling bifurcations, quasiperiodicity as well as intermittency, interior crisis, hyperchaos are only a few. In this work, strange attractors, bifurcation diagrams, periodic windows, invariant characteristics are investigated both analytically and numerically.

Keywords: 2-D nonlinear maps; chaos; quasiperiodicity; bifurcations; hyperchaos.

1. Introduction

Over the past few decades, scientists have come to understand that a large variety of systems exhibit complicated evolution both in space and time. Chaos is such a dynamic behavior that is, surprisingly enough, encountered in algebraically simple dynamical systems. In the case of discrete mappings, several examples of simple polynomial maps are thoroughly studied in the literature [Ott, 2002]. This is not the case though, with rational maps which, to our best knowledge, are thoroughly yet to be studied.

1.1. *Related literature and contribution*

The model we discuss in this paper, is

$$F\begin{pmatrix} x \\ y \end{pmatrix} = \begin{pmatrix} -\dfrac{ax}{1+y^2} \\ x + by \end{pmatrix} \tag{F}$$

where $a, b \in \mathbb{R}$ are the control parameters.

This map was first reported and studied in [Zeraoulia & Sprott, 2011a] in some detail. The study of (F) has also been proposed as an open problem in [Zeraoulia & Sprott, 2011b].

*The Institute For Systems Research, College Park, MD 20740, USA.

In this paper, we answer this call and study the problem, contributing some new analytical results as well as observations based on advanced numerical measurements. Despite, its simplicity, this map is rich in various nonlinear phenomena many of which are mathematically tractable. These types of rational models occur in the area of biological and evolutionary algorithms. A first example of a one-dimensional rational map $g_a(x) = \frac{1}{0.1+x^2} - ax$ is presented and discussed in [Lu *et al.*, 2004], as a result of the study of evolutionary algorithms. Furthermore, in [Chang, 2005], the authors proposed a two-dimensional version of $g_a(x)$: $h_{a,b}(x,y) = (\frac{1}{0.1+x^2} - ay, \frac{1}{0.1+y^2} + bx)$. We expect the study of (F) to pave the way for a unified theoretical framework suitable for these types of dynamical systems. This work is an outgrowth of [Somarakis & Baras, 2011a] from which some main simulation results are drawn.

1.2. *Paper structure*

The paper is organized as follows. In Sec. 2, we introduce notations and review the main definitions and theoretical framework to be used. In Sec. 3, we present simulations of the phase space for typical values of parameters a and b. These figures illustrate the state dynamics of (F) and shall be discussed throughout the paper. In Sec. 4, the analytical properties of the map are established. We emphasize the existence and stability of periodic solutions. Moreover, we state few useful propositions that outline the steady state dynamical behavior of the system for the parameter region $|b| < 1$. In Sec. 5, we make a thorough simulation analysis. Our goal will be to discuss the transition to chaos, to report and characterize bifurcations that take place as a increases through critical values (some of them already known from the analytical study). We also argue that a rather unusual quasiperiodicity involved scenario takes place as (F) becomes chaotic. In Sec. 5.2, we report and characterize some other nonlinearities such as coexistence of attractors, interior crises and hyperchaos. In Sec. 5.3, we estimate the Lyapunov spectrum and the correlation sums of the attractors of Sec. 2 whereas in Sec. 5.4, we briefly discuss the question whether (F) can have multiscroll chaotic attractors. We summarize and discuss our results in Sec. 6. In our effort to make this paper as self-contained as possible, we included two Appendices: one with related results from Center Manifold Theory and one discussing the Neimark–Sacker bifurcation (Hopf bifurcation for discrete time systems). Furthermore, we have omitted few but only technical steps in the proofs of our results. For complete proofs and detailed discussion of this work, see the technical report [Somarakis & Baras, 2011b].

2. Notations and Definitions

In this section, we will define the setting of (F) and we will review definitions from dynamical systems theory. The space we use is the standard planar Euclidean space $\mathbb{R}^2$ so that $x, y \in \mathbb{R}$, always. The parameters a, b are taken to be real, as well. By $q(w) = \mathcal{O}(e(w))$ we understand that there exist positive δ, M such that $|q(w)| \leq M|e(w)|$ for $|w| < \delta$.

Attractors and invariant manifolds

A commonly accepted definition of an attractor with respect to a dynamical system D is that of a D-invariant set $\mathcal{A}$ and an open neighborhood of this set, such that any solution starting in the open neighborhood will asymptotically converge to $\mathcal{A}$. Given a dynamical system D and a fixed point $\bar{x}$ such that $D\bar{x} = \bar{x}$, the stable and unstable manifolds of $\bar{x}$ are defined as follows

$$\mathcal{W}_N^{S,U}(\bar{x}) = \{x \in N(\bar{x}) : D^t x \to \bar{x} \text{ as } t \to \pm\infty\},$$

the global analogues of $\mathcal{W}_N^{S,U}$ are defined by letting points in $\mathcal{W}_N^S$ ($\mathcal{W}_N^U$) flow backward (forward) in time. For simplicity we will drop N, the symbol of locality. In many degenerate cases caused by critical parameter values, the emergence of a third type of invariant manifold, emerges, known as the center manifold, the notion of which is of great importance in the discussion of bifurcations (Appendix A).

2.1. *Nonlinear phenomena*

Let us now briefly review some nonlinear phenomena which we will encounter in our discussion of the dynamic behavior of (F). Most of these definitions are drawn from [Ott, 2002].

Coexistence of attractors

The coexistence of attractors is the phenomenon of multiple invariant sets (and consequently multiple open neighborhoods) for D. Extending the definition of $\mathcal{A}$ to include the point at infinity, similar

phenomena are observed in the behavior of (F) with $|b| > 1$.

Intermittent behavior

This behavior is associated with the irregularity of solutions of a system as its parameters are varied through a critical value. Below this value the behavior may be, for example, periodic while for values above, it is chaotic. The phenomenon is observed in the neighborhood of this critical value, where one observes stretches of time where the solution lies in one phase (periodic) and also where solution lies in the other phase (aperiodic). System (F) indeed exhibits such behavior which we outline and classify in Sec. 5.1.

Crises

Sudden changes in chaotic attractors with parameter variation are seen very commonly in the study of chaotic systems. They are usually caused by some collision of the chaotic attracting invariant set with an unstable invariant periodic orbit. The types of crises depend on the nature of the discontinuous change: in the *boundary crisis* the chaotic attractor is suddenly destroyed, in the *interior crisis* where the size of the attractor in phase space suddenly increases and in the *interior merging crisis* chaotic attractors simultaneously collide with a periodic orbit to form one chaotic attractor. In this work, an interior crisis is observed and numerically analyzed.

Hyperchaos

This phenomenon is associated with the existence of more than one positive Lyapunov exponents along a chaotic solution of a dynamical system. In our work, time-series analysis of (F) with $|b| > 1$ indeed reveals such solutions which are very interesting especially because the system is a very simple rational planar map. Such solutions were also reported in [Zeraoulia & Sprott, 2011a].

3. Orbit Simulations

In this section, we illustrate typical attractors of (F) for different values of (a, b). The results are presented in Fig. 10. The variety of the strange attractors motivates a further investigation of this dynamical system.

4. Analytical Approach

In this section, we will present rigorous results on the most important properties of (F), in the form of lemmas and propositions.

4.1. *First remarks*

The fact that the denominator of (F) is always greater than 1, makes the system $C^\infty(\mathbb{R}^2)$. Moreover, while (F) is an odd function of (x, y) (i.e. $F(-x, -y) = -F(x, y)$), the Jacobian matrix, at $(x, y) \in \mathbb{R}^2$.

$$DF(x,y) = \begin{pmatrix} \dfrac{-a}{1+y^2} & \dfrac{2axy}{(1+y^2)^2} \\ 1 & b \end{pmatrix} \tag{1}$$

is an even function of (x, y).

Given (x_0, y_0) the nth iterate of (F) is

$$\begin{aligned} \begin{pmatrix} x_{n+1} \\ y_{n+1} \end{pmatrix} &= F \begin{pmatrix} x_n \\ y_n \end{pmatrix} \\ &= F^{(n+1)} \begin{pmatrix} x_0 \\ y_0 \end{pmatrix} \\ &= \begin{pmatrix} \dfrac{(-1)^{n+1} a^{n+1}}{\prod_{i=0}^{n} (1+y_i^2)} x_0 \\ b^{n+1} y_0 + b^n \sum_{i=0}^{n} b^{-i} x_i \end{pmatrix} \end{aligned} \tag{2}$$

where $x_{n+1} = F^{(1)}(x_n, y_n), y_{n+1} = F^{(2)}(x_n, y_n)$.

It trivially follows from (2) that for $a > 0$, solutions oscillate between $\{(x, y) : x > 0\}$ and $\{(x, y) : x < 0\}$, while for $a < 0$ x_n preserves the sign of x_0. The next result responds to the boundedness of solutions.

Proposition 1. *For all $a \in \mathbb{R}$ and $|b| < 1$, all solutions of (F) are bounded. If $|b| > 1$ there are always unbounded solutions.*

Proof. For the second part of the statement, take $(0, y_0 \neq 0)$ and use (2) to obtain $x_n \equiv 0$ and $|y_n| = |b|^n |y_0| \to \infty$.

The first part of the proof occurs by contradiction. Assume that there exist (x_0, y_0) that generates a solution $\{x_k, y_k\}$ with a subsequence $|x_{k_i}| + |y_{k_i}| \to \infty$ for some strictly increasing sequence of

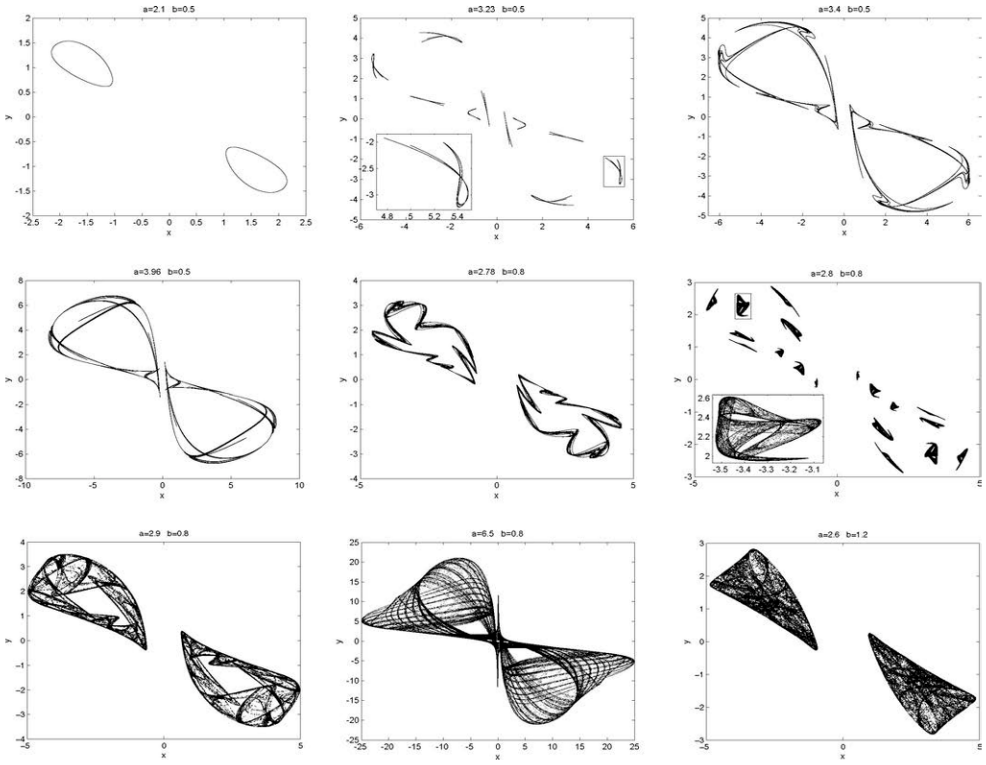

Fig. 1. Phase plots of (F) for various parameters. The title of each subplot carries the parameter values that generate the limit set. In the following, the notation Fig. $1_{(a,b)}$ will be used to enumerate the corresponding subplot.

naturals $k_i \to \infty$ as $i \to \infty$. We consider cases:

(1) $|y_k| \leq M < \infty$: Then x_k must admit an unbounded subsequence. However from (F)(b) it follows that $|x_k| \leq M(1 + |b|)$.
(2) $|x_k| \leq M < \infty$: Then from (2)(b) we have $|y_k| \leq |b|^k |y_0| + \frac{M}{1-|b|} < \infty$.
(3) $|x_{k_j}|, |y_{k_j}| \to \infty$: It follows that $\limsup |x_n| \geq |x_{k_i}| = \infty$ and of course $\sum_k |x_k| \geq \sum_j |x_{k_j}| = \infty$. From the ration test we have that

$$\frac{|x_{k+1}|}{|x_k|} = \frac{|a|}{1 + y_k^2} \geq 1 \tag{3}$$

must hold for infinitely many k's. Equivalently $|y_k| \leq \sqrt{|a| - 1}$ for infinitely many k's.

From (2)(b) and since $|b| < 1$, we have that

$$b^k \sum_{l=0}^{k} b^{-l} x_l < \infty \tag{4}$$

for infinitely many k. Then $\limsup_k \sum_l b^{-l} x_l$ either converges or it diverges as b^{-k}. Both these cases contradict the unboundedness of $|y_{k_j}|$. ■

4.2. *Fixed points*

The first result is summarized in the following proposition:

Proposition 2. *The fixed points of* (F) *are*

(1) $b \neq 1$, $a \leq -1$: $(0,0)$, $(\pm(1-b)\sqrt{-1-a}, \pm\sqrt{-1-a})$.
(2) $b \neq 1, a > -1$: $(0,0)$ *unique.*
(3) $b = 1$: *y-axis is a continuum of fixed points.*

Moreover,

(1) $(0,0)$ *is asymptotically stable if* $|a| < 1$ *and* $|b| < 1$,
(2) $(\pm(1-b)\sqrt{-1-a}, \pm\sqrt{-1-a})$ *are asymptotically stable if* $-2 < a < -1$ *and* $-\frac{7a+8}{a} \leq b < 1$.

Proof. The fixed points of (F) are the solution of the algebraic equation $F(x,y) = (x,y)$. Then, evaluating (1) around the solutions and calculating the eigenvalues we obtain the local stability bounds. Specifically if (x_0, y_0) is the origin and $(|x_1|, |y_1|) = (|(1-b)\sqrt{-1-a}|, |\sqrt{-1-a}|)$

$$DF_{(x_0,y_0)} = \begin{pmatrix} a & 0 \\ 1 & b \end{pmatrix},$$

$$DF_{(x_1,y_1)} = \begin{pmatrix} 1 & -2\dfrac{(1-b)(1+a)}{a} \\ 1 & b \end{pmatrix}.$$

The eigenvalues of $DF_{(x_0,y_0)}$ are a, b and those of $DF_{(x_1,y_1)}$ are $\frac{b+1}{2} \pm \frac{1}{2a}\sqrt{\Delta}$ where $\Delta = a(b-1)(ba+7a+8)$. Sufficient conditions for the local asymptotic stability of x_1, y_1 is the condition

$$\left|1 + b \pm \frac{\sqrt{\Delta}}{a}\right| < 2. \tag{5}$$

The stability bounds are established by taking cases for the sign of Δ and combining the resulting conditions with (5). This is a tedious algebraic exercise and can be found in [Somarakis & Baras, 2011b]. ■

This linearization analysis provides only sufficient conditions for local asymptotic stability. In case of $|a|, |b| < 1$, we have a much stronger result:

Proposition 3. *If* $|a|, |b| < 1$ *then the origin* $(0,0)$ *is globally asymptotically stable.*

Proof. For these parameters, Proposition 2 asserts that there are no other fixed points other than the origin. Also, for $|a| < 1$ there are no periodic solutions. Indeed if (x,y) solves $F^{(p)}(x,y) = (x,y)$ for some $p > 0$, then one can derive from (2)

$$(-1)^p a^p = (1+y_0^2)(1+y_1^2)\cdots(1+y_{p-1}^2) \tag{6}$$

which makes no sense for $|a| < 1$ as the left-hand side is less than one and the right-hand side is strictly larger than one. Finally, consider the Lyapunov candidate

$$V(x,y) = \kappa_1 x^2 + \kappa_2 y^2$$

for some $\kappa_{1,2} > 0$. Then throughout any solution (x_k, y_k):

$$\begin{aligned} \Delta V &= V(x_{k+1}, y_{k+1}) - V(x_k, y_k) \\ &= \left(\kappa_1 \frac{a^2}{(1+y_k^2)^2} + \kappa_2 - \kappa_1\right) x_k^2 \\ &\quad + 2\kappa_2 x_k y_k + \kappa_2(b^2-1) y_k^2 \\ &\leq (\kappa_1(a^2-1) + \kappa_2 + b^2) x_k^2 \\ &\quad + \kappa_2((b^2-1) + \kappa_2) y_k^2 < 0 \end{aligned}$$

whenever $0 < \kappa_2 < 1 - b^2$ and $\kappa_1 > \frac{b^2+\kappa_2}{1-a^2}$. ■

As a increases through 1 the origin loses its stability. We will see that new attracting sets appear while $(0,0)$ becomes a saddle point as long as $|b| < 1$. Moreover, it can be easily verified that the y-axis is the global stable manifold $\mathcal{W}^S(0,0)$ which the attracting sets approach as a increases but they never overrun it.

4.3. *Periodic solutions*

In Sec. 2, we argued that for $|a| < 1$ there are no periodic solutions. In view of (6) we establish the following proposition.

Proposition 4. *Fix* $|b| < 1$. *Then the following statements hold*:

(1) *if* $[(x_1, y_1), \ldots, (x_p, y_p)]$ *is a p-periodic solution, then so is* $[(-x_1, -y_1), \ldots, (-x_p, -y_p)]$,
(2) *if* $|a| \leq 1$ *there are no periodic solutions of period* $p \geq 2$,
(3) *if* $a > 1$ *there are no periodic solutions of odd period.*

Proof. (1) Follows readily from the observation that $F^{(p)}$ is an odd function for any $p > 0$ while parts (2) and (3) follow from Eq. (6). ■

The following two propositions describe the dynamics of (F) for fixed $|b| < 1$ when a increases through 1, its behavior in $(|b|, 2)$ and finally as a increases through 2.

Proposition 5. *For any $|b| < 1$, (F) exhibits a period-doubling bifurcation as a increases through 1.*

Proof. The proof follows the discussion in [Wiggins, 2003; Carr, 1981] for the bifurcations of fixed points of maps. For any fixed number $|b| < 1$ and $a \in (1-\epsilon, 1)$ the origin is a hyperbolic asymptotically stable fixed point which loses its hyperbolic nature as a reaches 1. A center manifold then emerges, the behavior of (F) characterizes the overall (F) (see [Carr, 1981, Theorem § 1.5]). For a more rigorous consideration, the Jordan canonical decomposition of (F) around $(0,0)$ is

$$\begin{pmatrix} x_{n+1} \\ y_{n+1} \end{pmatrix} = \begin{pmatrix} -a & 0 \\ 1 & b \end{pmatrix} \begin{pmatrix} x_n \\ y_n \end{pmatrix} + \begin{pmatrix} ag(x_n, y_n) \\ 0 \end{pmatrix}$$

with $g(x,y) := \sum_{l\geq 1}(-1)^{l+1} x y^{2l}$. Since $b + a \neq 0$ for a close enough to 1, we consider the transformation $u_n := \frac{x_n}{b+a}$, $v_n := \frac{x_n}{b+a} + y_n$ and the system is written as

$$\begin{pmatrix} u_{n+1} \\ v_{n+1} \end{pmatrix} = \begin{pmatrix} -a & 0 \\ 0 & b \end{pmatrix} \begin{pmatrix} u_n \\ v_n \end{pmatrix} + a \begin{pmatrix} g(u_n, v_n) \\ g(u_n, v_n) \end{pmatrix}.$$

Note that x, y close to $(0,0)$ is equivalent to u, v close to $(0,0)$. The center manifold of the origin is

$$\mathcal{W}^C_{(0,0)} = \{(u,v) \in \mathbb{R}^C \times \mathbb{R}^S : v = h(u), |u| < \delta, \\ h(0) = Dh(0) = 0\}.$$

From the above definition, h is assumed to be of order $\mathcal{O}(u^2)$ near the origin. It can then be calculated that $g(u, h(u)) = -u^3 + \mathcal{O}(u^4)$ and the stability function of (F) on $\mathcal{W}^C$ is

$$u_{n+1} = -au_n - au_n^3 + \mathcal{O}(u_n^4) =: f(u_n, a). \quad (7)$$

The bifurcation of (7) at $a = 1$ is then equivalent to the bifurcation of (F) [Wiggins, 2003, § 21]. Finally, the sufficient conditions for a period-doubling bifurcation [Wiggins, 2003, § 21.2B] are:

$$\begin{aligned} f = 0, \quad f_u = -1, \quad f^{(2)}_a = 0, \\ f^{(2)}_{uu} = 0, \quad f^{(2)}_{ua} = -2, \quad f^{(2)}_{uuu} = 2 \end{aligned} \quad (8)$$

all evaluated at $(0,1)$, $a = 1$. Finally $-f^{(2)}_{ua}/f^{(2)}_{uuu} > 0$ implies that a period 2 bifurcation occurs for fixed $|b| < 1$ and a increasing through 1. ■

Lemma 1. *For any $1 < a < 2, |b| < 1$, (F) has a unique period 2 orbit $(\mp(b+1)\sqrt{-1+a}, \pm\sqrt{-1+a})$ which is locally asymptotically stable.*

Proof. Locality directly emerges from the existence of other invariant solutions such as the zero one. The period two solutions satisfy $F^{(2)}(x,y) = (x,y)$ so that

$$\begin{aligned} (1+y^2)(1+(x+by)^2) = a^2 \\ \frac{-ax}{1+y^2} + b(x+by) = y \end{aligned} \quad (9)$$

where solving the second for x and substituting in the first, the equations yield

$$t^4 + c_3 t^3 + c_2 t^2 + c_1 t + c_0 = 0$$

where $t = y^2$, $c_0 = b^2 + a^2(1-b^2) - a^4 - 2ba + 2a^3 b$, $c_1 = 3b^2 + 2a^3 b + a^2(1-b^2) - 6ab + 1$, $c_2 = 3b^2 - 6ab + 3$, $c_3 = b^2 - 2ba + 3$. Using MAPLE, the solutions are $t_{1,2} = -1 \pm a$, $t_{3,4} = \frac{2ba - b^2 - 1}{2} \pm \frac{1}{2}\sqrt{(1-b^2)(1-(2a-b)^2)}$. For $a > 1, |b| < 1$ only t_1 yields a positive, thus acceptable solution. Finally $y = \pm\sqrt{t_1}$ and use any of (9) to obtain x's. The local stability of the periodic solution occurs again by linearization and inspection of the eigenvalues of the matrix

$$DF_{(x_1,y_1)} DF_{(x_2,y_2)} = \begin{pmatrix} \dfrac{(1+2b)(1-a)+1}{a} & \dfrac{2(1-b^2)(a-1)}{a} \\ -1+b & -\dfrac{2(b+1)(a-1)}{a} + b^2 \end{pmatrix}$$

which are

$$\frac{2}{a} - \frac{3 - 4b - b^2}{2} \pm \frac{1}{2a}\sqrt{a(1+b)(b-1)^2(ba+8-7a)}.$$

It is shown in [Somarakis & Baras, 2011b] that for the given parameter values, these eigenvalues lie inside the unit circle. ■

The next proposition discusses perhaps the most interesting nonlinear phenomenon of (F).

Proposition 6. *For any $|b| < 1, b \neq 0$, (F) exhibits a supercritical Neimark–Sacker bifurcation as a increases through* 2.

Proof. The periodic solution of F is the fixed point of F^2 which by the above lemma has proved to be locally asymptotically stable for $|b| < 1$ and $a \in (1, 2)$. We will consider only one of the fixed points of $F^{(2)}$ as the dynamics are identical. Let this be $(\bar{x}, \bar{y}) = (-(1+b)\sqrt{a-1}, \sqrt{a-1})$. It suffices to prove that $F^{(2)}$ bifurcates at $a = 2$ in the sense of Neimark–Sacker (or discrete Hopf). This bifurcation is verified by applying Theorem 3.5.2 of [Guckenheimer & Holmes, 2002] also cited in Appendix B. In order to apply this theorem, however, certain transformations and calculations need to be done in (F).

Fix $b \in (-1, 0) \cup (0, 1)$. Consider the transformations $\bar{x} := \frac{2}{b+1}(x - \bar{x}) + (y - \bar{y})$, $\bar{y} := \frac{K}{a(b+1)} \times (y - y)$ where $K := \sqrt{a(b+1)|ba + 8 - 7a|}$.

The normal form of $F^{(2)}$ around $(\bar{x}, \bar{y})$ creates the form that can be used to apply the Theorem in Appendix B. Calculations done in [Somarakis & Baras, 2011b] yield

$$\begin{pmatrix} \hat{x} \\ \hat{y} \end{pmatrix} \to D \begin{pmatrix} \hat{x} \\ \hat{y} \end{pmatrix} + \begin{pmatrix} f_1(\hat{x}, \hat{y}) \\ f_2(\hat{x}, \hat{y}) \end{pmatrix} \tag{10}$$

where D is the diagonal matrix with elements, the eigenvalues of the linearized around $(\bar{x}, \bar{y})$ map $H(x - \bar{x}, y - \bar{y}) := F^{(2)}(x - \bar{x}, y - \bar{y}) - (\bar{x}, \bar{y})$. The eigenvalues are $\lambda = \frac{2(b+1)}{a} - \frac{3}{2} - 2b + \frac{b^2}{2} + \frac{i|b-1|}{2a}K$ and $|DH(0)| = \frac{(ba+2a-2-2b)^2}{a^2}$. Finally, $f_1(\hat{x}, \hat{y}) = \frac{2}{b+1}H_1(\frac{K}{2a}\hat{x} - \frac{1+b}{2}\hat{y}, \hat{y}) + H_2(\frac{K}{2a}\hat{x} - \frac{1+b}{2}\hat{y}, \hat{y})$ and $f_2(\hat{x}, \hat{y}) = \frac{K}{a(b+1)}H_2(\frac{K}{2a}\hat{x} - \frac{1+b}{2}\hat{y}, \hat{y})$.

At first note that for $\frac{8}{7-b} < a < 2$ the eigenvalues are complex conjugate and at $a = 2$, the first eigenvalue of D is

$$\lambda(a = 2) = \frac{1}{2}b^2 - \frac{1}{2} - b + \frac{i}{2}\sqrt{(1 + b)(3 - b)(b - 1)^2} \tag{11}$$

where $|\lambda(a = 2)| = \sqrt{|DH(0)|} = \sqrt{\frac{(ba+2a-2-2b)^2}{a^2}} = 1$. Also all powers of $\lambda^k(a = 2)$ are different than 1 for $b \neq 0$ (it holds that $\lambda^3(a = 2)|_{b=0} = 1$). Also

$$\frac{d}{da}|\lambda(a = 2)| = -\frac{(1 + b)(b^2 - 2b + Z + 1)}{2Z} \tag{12}$$

where $Z =: \sqrt{(1 + b)(3 - b)(b - 1)^2}$. Calculations are tedious and they were carried out in MAPLE (see [Somarakis & Baras, 2011b]). The results yield $\xi_{20} = \frac{b^2-5b+6}{8} - i\frac{b(3-b)^{3/2}}{8\sqrt{1+b}}$, $\xi_{11} = 0$, $\xi_{02} = \frac{b^2-3b}{8} + i\frac{b(3-b)^{3/2}}{8\sqrt{1+b}}$, $\xi_{21} = \frac{(5+b)\sqrt{3-b}}{16\sqrt{1+b}} + i\frac{3(1-b)}{16}$. So S reads

$$\begin{aligned} S &= -|\xi_{02}|^2 + \mathrm{Re}\{\bar{\lambda}\xi_{21}\} \\ &= -\frac{b^3(b-3)^2}{65 + 65b} + \frac{1}{16}\frac{(5 + b)\sqrt{3 - b}}{\sqrt{1 + b}} \\ &\quad + \frac{3}{32}\sqrt{(1 + b(b - 1)(3 - b))^2(1 - b)}. \end{aligned} \tag{13}$$

The two plots in Fig. 2 indicate that S is not zero for $|b| < 1$. Moreover, the signs of $S(b)$ and $\frac{d\lambda(a=2)}{da}$ in this interval imply that the bifurcation as a increases through 2 is supercritical and thus the emerging invariant set is attracting, which is in agreement with the numerical findings. This concludes our proof. ■

4.3.1. *Stability of periodic solutions and coexistence of attractors*

Periodic solutions are all the (x, y) that satisfy $F^{(p)}(x, y) = (x, y)$ for some integer $p > 1$. The following result establishes the interesting nonlinear phenomenon of the coexistence of attractors.

Proposition 7. *Consider (F) with $a > 0$ and $|b| < 1$. If a p-periodic solution is locally asymptotically stable (unstable) then so is its opposite one.*

Proof. From Proposition 3.1, we proved that if there exists a period-p solution $\{(x_1, y_1), \ldots, (x_p, y_p)\}$ then $\{(-x_1, -y_1), \ldots, (-x_p, -y_p)\}$ is another one. The result follows trivially from the fact that (1) is an even function of (x, y) and will be any p-product, so that the local dynamics of the two periodic solutions are identical. ■

Note that for the case $p = 2$ there is only one periodic solution because the two solutions coincide.

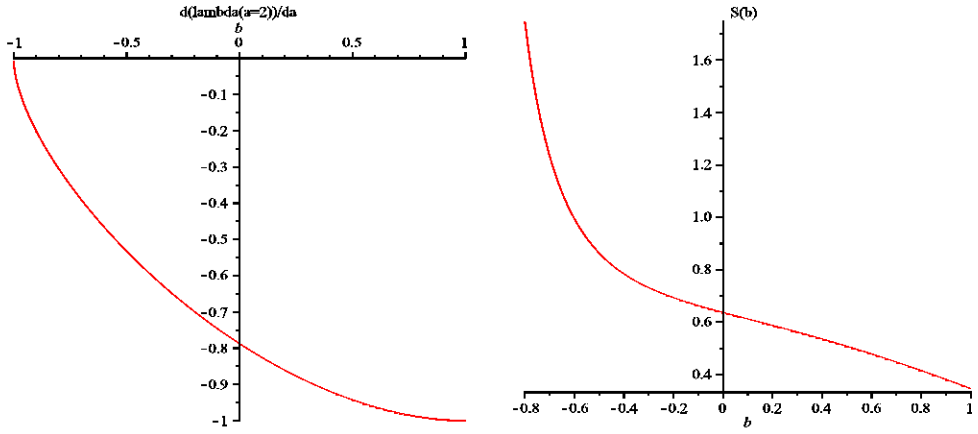

Fig. 2. The plots of $\frac{d}{da}\lambda(a=2)$ and S as functions of b.

However, this is not typical. In Fig. 6(a), we numerically verify the existence and stability of other periodic solutions.

4.3.2. *The case $a > 0, -1 < b \leq 0$*

Although this range of values for b is not of main interest; we devote this section to few interesting results when b takes negative values. The next lemma tells us that the subset

$$U = \left\{(x,y) \in \mathbb{R}^2 : xy < 0, 1 + \frac{1}{a}\frac{x}{y} > 0\right\} \tag{14}$$

is F invariant and positively attracting.

Lemma 2. *Assume (F) with $a > 0, -1 < b \leq 0$. Then $\forall\ (x_0, y_0) \in \mathbb{R}^2 : x_0 \neq 0\ \exists N = N(x_0, y_0, a, b) : (x_n, y_n) \in U\ \forall n \geq N$. Moreover, $x_0 y_0 \in U$ implies $x_n y_n \in U\ \forall n \geq 0$.*

Proof. Consider the set $\Omega = \{(x,y) \in \mathbb{R}^2 : xy < 0\}$. We have

$$\begin{aligned} x_{n+1}y_{n+1} = {} & x_{n+1}b^{n+1}y_0 + x_{n+1}x_n + x_{n+1}x_{n-1}b \\ & + x_{n+1}x_{n-2}b^2 + \cdots + x_{n+1}x_0 b^n. \end{aligned} \tag{15}$$

Inspecting (F)(a) we observe that all, but first, terms on the right-hand side of (8) are negative. Since from Proposition 1, solutions are bounded, choosing N large enough (e.g. $N > 1$ such that $b^{N+1}y_0 \prod_{i=0}^{N-1}(1+y_i^2) \leq (-1)^N a^N x_0$), the first part follows. For the second part of the lemma, consider the case $x_0 > 0, y_0 < 0$ then $x_1 < 0, y_1 > 0$ such that $x_1 y_1 < 0$. Assume that this holds for n. Then

$$x_{n+1}y_{n+1} = \frac{-ax_n^2 - abx_n y_n}{(1+y_n^2)} < 0. \tag{16}$$

Proving the statement by induction, similarly, for $x_0 < 0, y_0 > 0$, we showed that Ω is invariant and positively attracting. Now, consider U which is a subset of Ω. If $x_m y_m < 0$ for some $m \in \mathbb{N}$ then $(x_n, y_n) \in U\ \forall n \geq m+1$ since

$$\begin{aligned} 1 + \frac{1}{a}\frac{x_{m+1}}{y_{m+1}} &= 1 + \frac{1}{a}\frac{-ax_m}{1+y_m^2}\frac{1}{x_m + by_m} \\ &= 1 - \frac{1}{1+y_m^2}\frac{\frac{x_m}{y_m}}{\frac{x_m}{y_m} + b} > 0. \end{aligned}$$

Finally we show that U is attracting. Write

$$\begin{aligned} 1 + \frac{1}{a}\frac{x_{n+1}}{y_{n+1}} \geq 1 &- \frac{|b|^{n+1}}{a}\frac{|y_0|}{|y_{n+1}|} \\ &- \frac{|b|^n}{a}\sum_0^n |b|^{-i}\frac{|x_i|}{|y_{n+1}|}. \end{aligned}$$

Since, by Proposition 1, all solutions are bounded, the terms $|b|^n$ dominate for n large enough, so that

the right-hand side becomes positive. Since U is a subset of Ω the result follows. ■

Next we show that (F) restricted in U is a local diffeomorphism.

Proposition 8. *(F) is invertible along any solution such that $(x_0, y_0) \in U$ and consequently bijective in the forward limit set of (x_0, y_0).*

Proof. By the previous lemma, any solution will enter and remain in U. Given $(x_{n+1}, y_{n+1}) \in U$ such that $(x_{n+1}, y_{n+1}) = F(x_n, y_n)$ one can determine x_n, y_n solving (F) to obtain

$$y_n = \frac{ab \pm \sqrt{a^2b^2 - 4(x_{n+1} + ay_{n+1})x_{n+1}}}{2x_{n+1}}. \quad (17)$$

If $x_{n+1} > 0$, then $y_{n+1} < 0$ by assumption $-4(x_{n+1} + ay_{n+1})x_{n+1} > 0$, so that y_n attains one positive and one negative root. By invariance of U throughout the solution, we must choose the positive one. Similarly, if $x_{n+1} < 0$, we must accept the negative y_n. In any case $x_n = y_{n+1} - by_n$. So (F) is invertible along a solution. Since the forward limit set must lie in U, as both positive and negative invariants, (F) restricted to it, is a bijection which is differentiable in any compact subset of U. ■

5. Simulation Study

In this section, we study the rational map from a basically simulation point of view. This allows us to be more flexible in our observations and to discuss different transitions from period to chaos as well as various interesting nonlinear phenomena. We will mainly focus on the range of b which guarantees bounded solutions.

5.1. *Transition to chaos for $|b| < 1$*

Here, we present and discuss some numerical results of the types of chaotic transitions of (F) and try to interpret the findings that are theoretically consistent. Numerical evidence suggests that one route to chaos is via the typical period-doubling cascade (see Fig. 2). It is also claimed that chaos may occur via a quasiperiodic torus break down [Zeraoulia & Sprott, 2011a]. It is true that the quasiperiodic behavior of the system is ubiquitous on the (a, b) plane and it is reasonable to investigate the possibility that (F) follows the Ruelle–Takens–Newhouse route to chaos [Newhouse *et al.*, 1978]. Another chaotic transition that is reported is via intermittency. The chapter is almost exclusively devoted to the case $|b| < 1$. The routes to chaos for $|b| > 1$ are yet to be studied.

5.1.1. *Bifurcation diagram*

A bifurcation diagram for the fixed value of $b = 0.5$ and $a \in (1.8, 4.2)$ is presented in Fig. 3. From the discussion so far, we suspect that for $|b| < 1$, any bifurcation diagram is qualitatively similar for a significant part of the range of parameter a. Indeed, for $a \in (-1, 1)$ the origin is asymptotically stable while for $a \in (1, 2)$ a period 2 orbit becomes stable. As a increases through zero, a Neimark–Sacker bifurcation leads to quasiperiodicity. If one imagines the phase space of (F) as a Poincaré section, on a plane manifold embedded in the 3-D space, the period 2 and the Neimark–Sacker bifurcations correspond to two subsequent Hopf bifurcations of the abstract continuous system. Note also that as a increases so does the magnitude of the attractor. As long as $|b| < 1$ the solutions remain bounded. Due to the coexistence of attractors we expect that different initial conditions will yield different bifurcation diagrams.

5.1.2. *Quasiperiodic destruction → period doubling → chaos*

According to the Ruelle–Takens–Newhouse quasiperiodic route to chaos [Newhouse *et al.*, 1978], if a continuous system undergoes three subsequent Hopf bifurcations, then it is "likely" that the system possesses a strange attractor right after the third bifurcation. When the third frequency is about to occur, some broad band noise will simultaneously appear, if there is a strange attractor. Practically, the three tori can decay into a strange attractor immediately after the critical parameter value for its existence has been reached such that one observes in the power spectrum only two independent frequencies, that is, two Hopf bifurcations and then chaos. This is not exactly what we observe for (F) when $|b| < 1$. A typical chaotic transition of (F) is presented in Fig. 4. As a increases, the quasiperiodic attractor [Fig. 4(a)] folds and degenerates continuously [Fig. 4(c)] to a periodic attractor [Fig. 4(d)]. Then as we continue to increase a, a period-doubling cascade process leads to chaos [Figs. 4(e) and 4(f)]. This is not what we should expect according to theory [Newhouse *et al.*, 1978]. Quasiperiodic attractors occur for an abundance of values (a, b), however for $|b| < 1$ they appear to degenerate according to

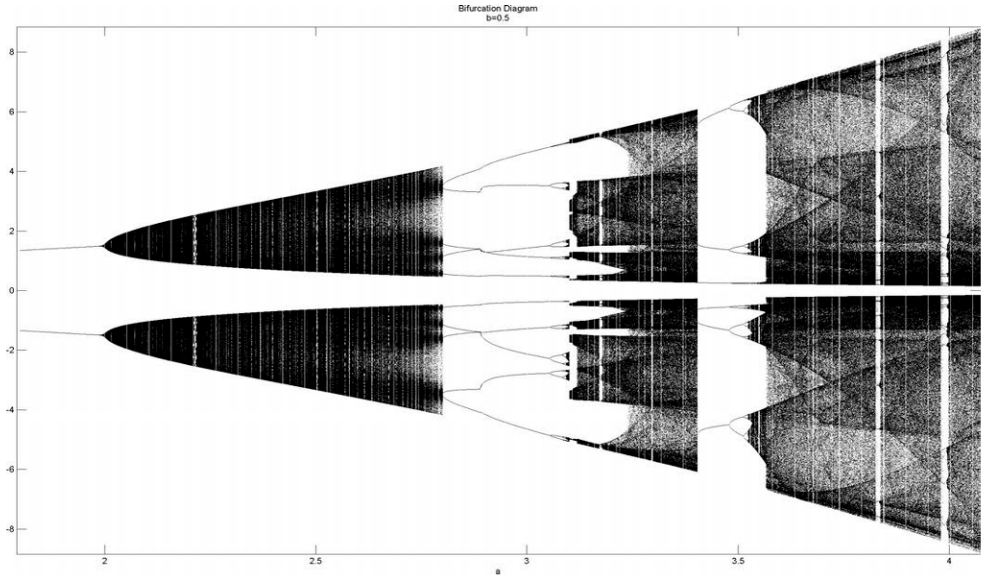

Fig. 3. Bifurcation diagram for $b = 0.5$ and $a \in (1.8, 4.2)$ and $(x_0, y_0) = (0.1, 0.1)$. At $a = 2$, a Neimark–Sacker bifurcation occurs bringing the system to quasiperiodic behavior.

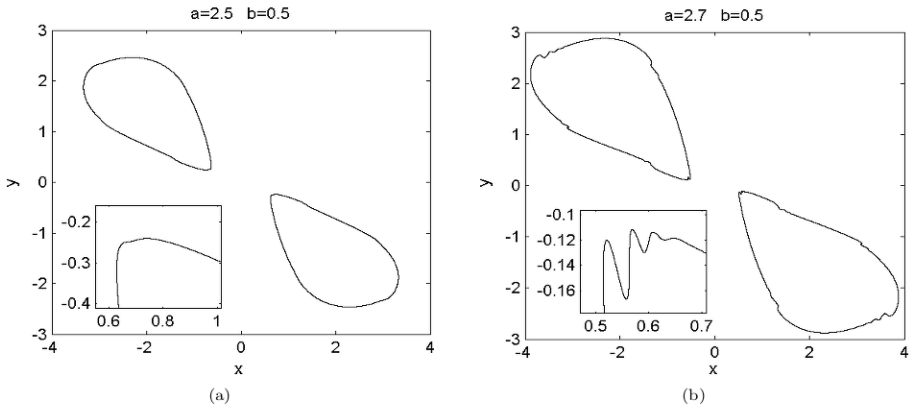

(a) (b)

Fig. 4. Chaotic transition via destruction of quasiperiodicity. All simulations suggest that a period-doubling cascade intervenes between quasiperiodic and chaotic dynamics.

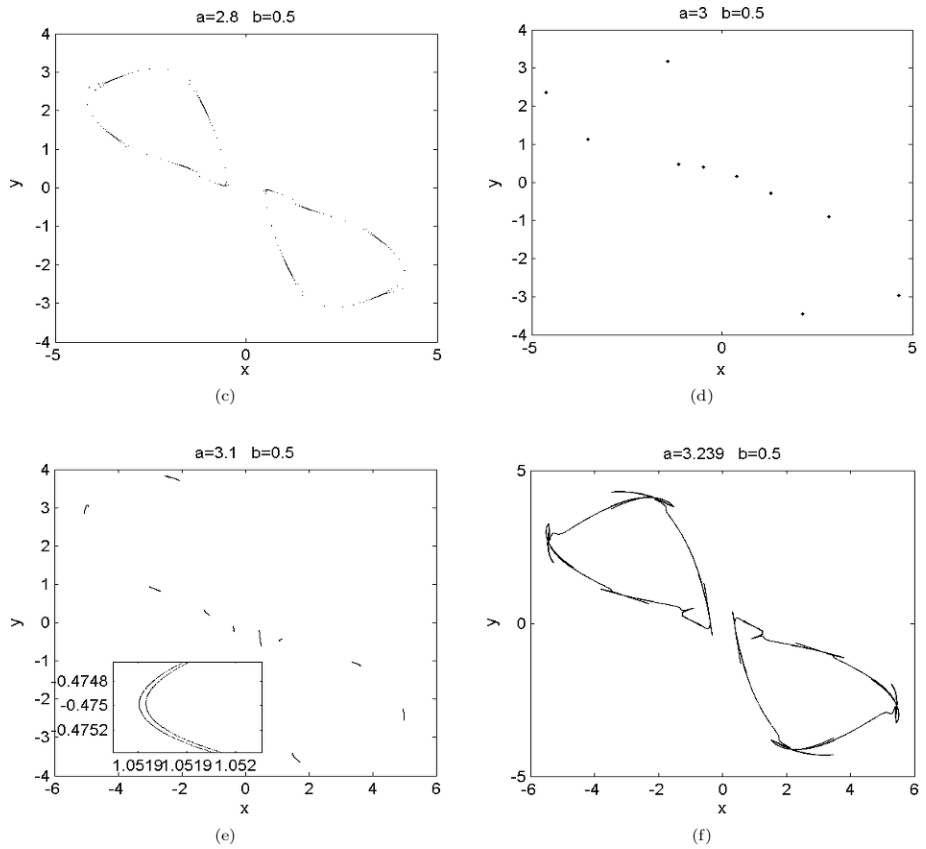

(c) (d) (e) (f)

Fig. 4. (*Continued*)

the description of Fig. 4. Strange attractors occur and in many cases they take the place and shape of a previous quasiperiodic attractor. We claim though that the transition follows a classical cascade.

5.1.3. *Transition to chaos through intermittency*

Intermittency is a regime with long-lived nearly periodic phases interrupted by nonperiodic bursts. This regime results from collision of stable and unstable periodic cycles. In the intermittent transition, one has a simple periodic orbit which is replaced by chaos as a parameter of the system passing through some critical value. This necessarily implies that the stable attracting periodic orbit either becomes unstable or it is destroyed. When this happens, the orbit is not replaced by another nearby stable periodic orbit, as occurs, for example, in the forward period-doubling bifurcation; this is implied by the fact that during the bursts, the orbit goes far from the vicinity of the original periodic orbit. The types of generic bifurcations which meet these requirements are the saddle-node

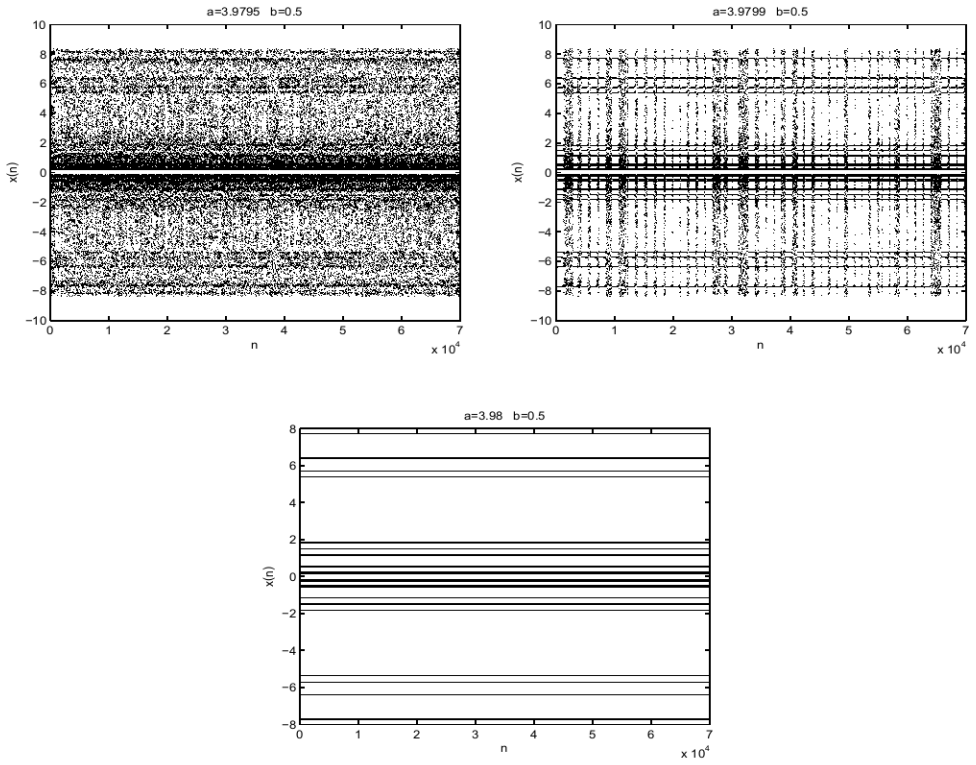

Fig. 5. The time-series plots (x_n, n) reveal chaotic transition via intermittency. Here $b = 0.5$ and $a_c \approx 3.9799$.

bifurcation, the inverse period-doubling bifurcation and the subcritical Neimark–Sacker bifurcation.

5.1.4. *Intermittent behavior at* $b = 0.5$, $a_c \approx 3.9979908$

In Fig. 5, we report such a transition for fixed $b = 0.5$ and a decreasing through 3.98 (period 26) to 3.9795 (chaotic). The plots are the time series (x_n, n) depicting the intermittency. Following [Ott, 2002; Pomeau & Manneville, 1980] and assuming that $a_c \approx 3.9979908$ is the critical value above which (F) behaves periodically and below which it enters a periodic-chaotic phase transition, the mean time between bursts $\overline{T}(a)$ as a approaches a_c from below diverges,

$$\lim_{a \to a_c^-} T(a) = +\infty.$$

In [Pomeau & Manneville, 1980], three types of intermittency transitions were classified each of which corresponds to a type of generic bifurcation:

(1) Type I: saddle-node, in which case $\overline{T}(a) \sim (a_c - a)^{-1/2}$ as $a \to a_c^-$
(2) Type II: Hopf, in which case $\overline{T}(a) \sim (a_c - a)^{-1}$ as $a \to a_c^-$

(3) Type III: inverse period doubling, in which case $\overline{T}(a) \sim (a_c - a)^{-1}$ as $a \to a_c^-$

A first step towards identifying the type of intermittency in Fig. 5 is to measure $\overline{T}(a)$ in the vicinity of a_c. This is depicted in Fig. 6 where plots of 10 000 000 steady-state iterations (after 1000 000 transient iterations) were generated for fixed $b = 0.5$ and parameter values of $a = 3.97990740285$, 3.9799074029, 3.979907402901, 3.979907402902, 3.979907402903, 3.979907402904, 3.979907402905, 3.979907402906, 3.979907402907, 3.979907402908, 3.979907402909, 3.97990740291. From Fig. 6 we observe that the scaling gives a slope that is calculated to be around 0.54. This indicates a Type I intermittency as a result of a saddle-node bifurcation. A more rigorous analysis of the nature of the transitions to chaos would require elaborate mathematical tools from Renormalization theory.

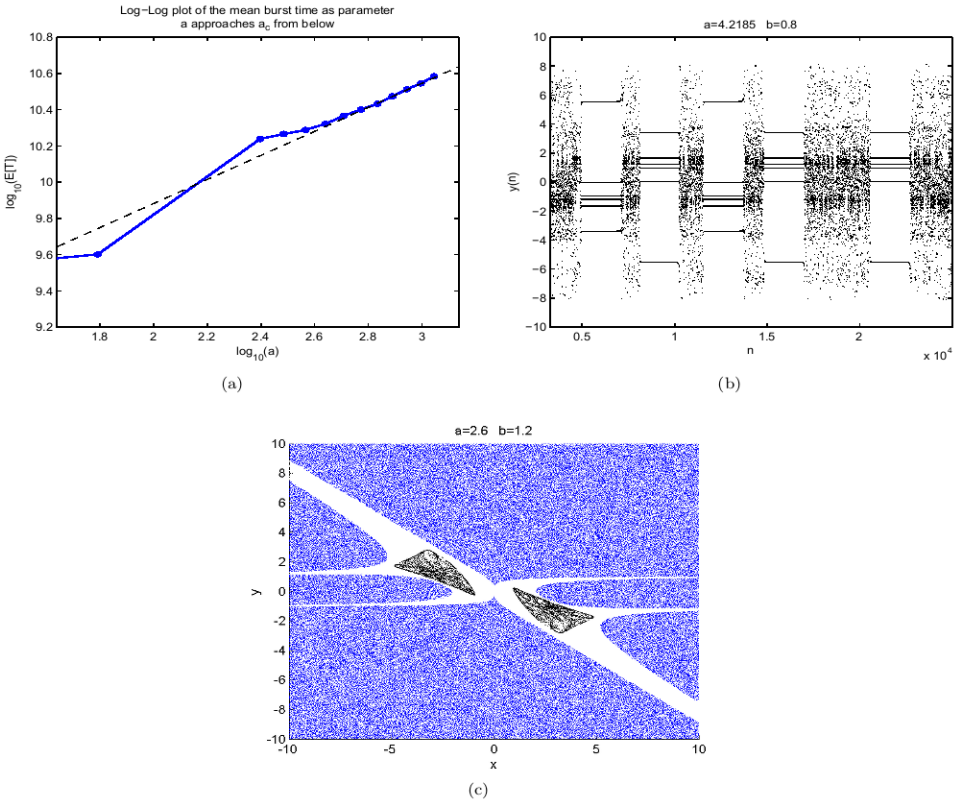

Fig. 6. Chaotic transition via intermittency. (a) The log–log plot of the mean burst time and the rescaled parameter a. As a approaches a_c from below there is clear scaling behavior. The slope of the line is calculated around 0.54. (b) Complex intermittent behavior. The orbit oscillates between chaotic and periodic behavior of two anti-symmetric periodic solutions, showing the phenomenon of coexistence of periodic attractors, already discussed in Proposition 5. (c) Coexistence of attractors for $|b| > 1$. The plot outlines the basin of attraction of the hyperchaotic attractor Fig. $1_{(2.6,1.2)}$ also presented here. The shaded region is the basin of attraction for the point at infinity, while the white region is the basin of the strange attractor.

5.2. *Other nonlinear phenomena*

In this section we discuss secondary nonlinear phenomena observed during the numerical speculation of the dynamics of (F) as well as some semi-rigorous discussion on the size of its attractors.

5.2.1. *Coexistence of attractors and hyperchaos*

From the discussion, the attractors coexist for both $|b| < 1$ and $|b| > 1$. In the first case, Proposition 6 reveals the existence of multiple periodic attractors; a result numerically verified in Fig. 6(b).

We know that for $|b| < 1$, the unique fixed point at the origin admits a global stable manifold $\mathcal{W}^S(0,0) := \{(x,y) \in \mathbb{R}^2 : x = 0\}$. For $|b| > 1$, $\mathcal{W}^S(0,0)$ vanishes to $(0,0)$ becoming actually a "stable manifold" of the point at infinity. Solutions then may become unbounded although there are attractors both nonchaotic and chaotic, depending on the value a. This is phenomenon of the coexistence of attractors. The strange attractors in Figs. $1_{(2.5)}$ and $1_{(2.6,1.2)}$ are in the area of $|b| > 1$. Note that Fig. $1_{(2.6,1.2)}$ is in fact hyperchaotic (i.e. both Lyapunov exponents are positive — see Table 1).

5.2.2. *Interior crisis at $a_c = 3.5657$, $b = 0.5$*

Among the ubiquitous nonlinear behavior are the crises. Here we report an interior type of crisis that occurs for $b = 0.5$ at the vicinity of $a_c := 3.5657$. As a increases through a_c the orbit on the attractor spends long stretches of time in the region to which the attractor was confined before the crisis. At the end of one of these stretches, the orbit bursts out of the old region and bounces around chaotically in the new enlarged region made available to it, by the crisis.

5.2.3. *On the size of the attractors*

In this final subsection we take the opportunity for a heuristic discussion on the size of the attractors for large values of a. A visual inspection of the bifurcation diagram in Fig. 2 reveals that the attractors' increase in size as they approach $(0,0)$ for large values of a. The latter is easy to study analytically. Take for simplicity $b = 0$ and initial data $(x_0 > 0, y_0 = 0)$. Then

$$x_3 = \frac{-a^3 x_0}{(1+x_0^2)(1+x_1^2)} \propto a^{-1}, \quad a \gg 1$$

as $y_2 = x_1 \propto a^2$. Working with (2), one obtains $y_3 = x_2 \propto a^2$ and finally

$$x_4 \propto a^{-2}, \quad y_4 = x_3 \propto a^{-1}.$$

In this section, we derive some bounds on this size, i.e. extreme values of x and y, as functions of the parameters a and b. We wish to find (x_0, y_0) so as to maximize $|x_2|$. Since the dynamics of (F) favor an expansion of $|x|$ by a factor of at most a, we suspect that it would be a good idea to exploit its maximum value. So we would choose $y_0 = 0$ and optimize x_0. The first iteration gives $x_1 = -ax_0$, $y_1 = x_0$ and the second $x_2 = a^2 x_0^2/(1+x_0^2)$, $y_2 = x_1 + bx_0$. Now $|x_2|$ is maximized at $x_0 = 1$ and in such case $x_3 = -\frac{a}{1+(a+b)^2}\frac{a^2}{2}$ which yields $|x_3| < |x_2|$ for $a > 1$ so that indeed the maximum value is attained in $x_2 = \frac{a^2}{2}$ and the extreme pair is $(\frac{a^2}{2}, b-a)$.

A drawback of this argument is that $(1,0)$ need not be a point of the attractor, not even close to it. Indeed, for small values of a this bound is not correct. However as $a \gg 1$ and b small enough (e.g. $\propto a^{-\mu} \to 0$) for some $\mu > 1$, the point $(1,0)$ gets closer to the attractor. This can be deduced from the fact that as $|b| < 1$ and in fact very close to zero, the global stable manifold $\mathcal{W}^S(0,0)$ attracts orbits to the origin for a fairly long time, linearization around the origin yields eigenvectors $\xi_1 = (0,1)^T$ (stable), $\xi_2 = (b+a,-1)^T$ (unstable). So as a gets larger the unstable eigendirection will get closer to the x-axis, approaching $(1,0)$.

Then, by a continuity argument of (F), such bound is valid. By symmetry $(-\frac{a^2}{2}, a-b)$ is also an extremal bound. Note that the above points are essentially bounds of the range of x. One more iteration yields bounds for $|y|$. Since $y_{n+1} = x_n + by_n$, one may deduce that the main contribution of the maximization of $|y|$ should come from a large enough $|x|$, especially for small b and large a. So starting from $(1,0)$ we get $x_3 = -\frac{a^3}{2(1+(b-a)^2)}$, $y_3 = \frac{a^2}{2} + b(b-a)$. All in all, we have argued that

$$X = \left\{(x,y) : |x|, |y| \le \frac{a^2}{2}\right\} \tag{18}$$

is the smallest positively invariant rectangle as $a \gg 1$ and b small enough. This heuristic approach

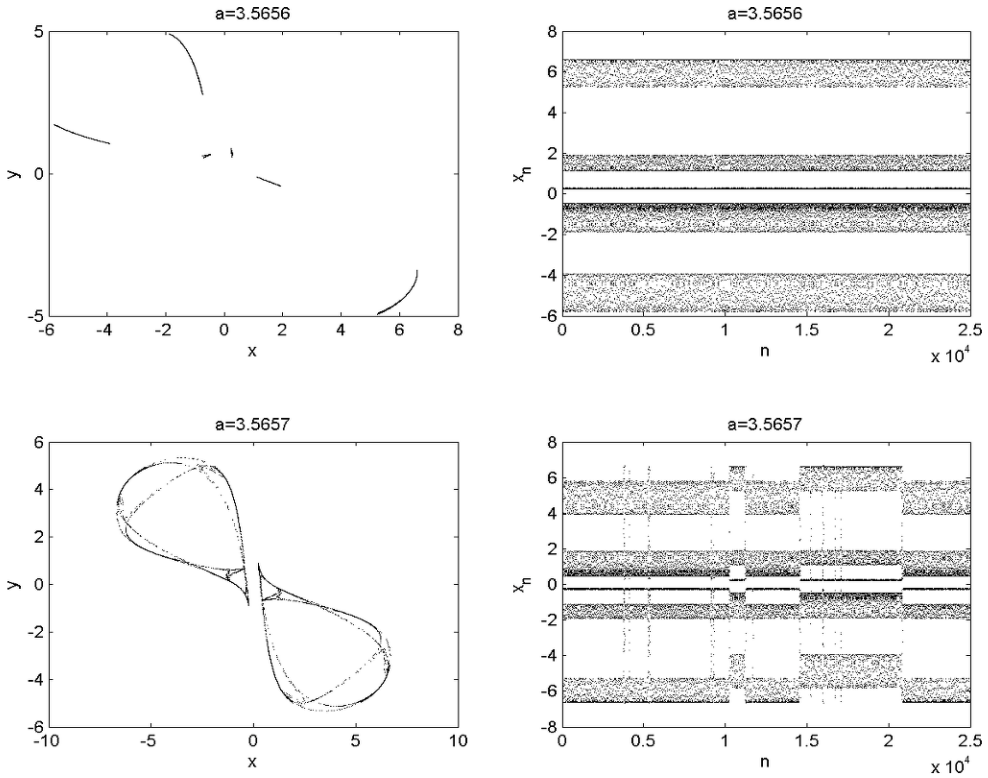

Fig. 7. Interior crisis. A sudden and significant increase in size and shape of the attractor as a passes through a_c.

is validated numerically and it holds for strange attractors obtained for $a > 1500$ and $b < \frac{1}{10a}$. Figure 7 illustrates the claims above.

5.3. *Exponents, dimensions, entropies*

In this section, we will discuss the characteristic invariants of the chaotic behavior of (F).

5.3.1. *Time series analysis*

In this section, we present numerical results of the main invariant characteristics of the attractors illustrated in Fig. 1, mainly for consistency. The three measures we approximate are the Lyapunov spectrum, the correlation dimension and the correlation entropy as these are the easiest and most appropriate for strange attractors to compute. Assuming that a natural F-invariant measure exists, the correlation sums were first introduced by Grassberger and Procaccia [1983]

$$C(m, \varepsilon, N) = \frac{2}{N(N-1)} \sum_{i=1}^{N} \sum_{j=i+1}^{N} \Theta(\varepsilon - \|\mathbf{x}_i - \mathbf{x}_j\|_m) \tag{19}$$

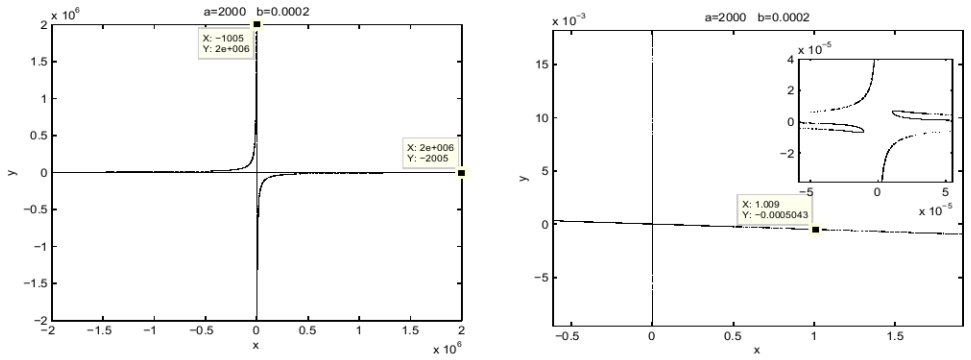

(a) (b)

Fig. 8. The size of attractors. Orbit of $F_{2000,0.0002}$. (a) The limits of the strange attractor are pointed out with data tips verifying the heuristic discussion. (b) A refined picture of the origin as well as a data tip of the point of the simulated orbit which presumably belongs to the attractor, that is also close to $(1, 0)$.

where Θ is the Heavyside step function, m the embedding dimension [Kantz & Schreiber, 1999]. So $C(m, \varepsilon, N)$ counts the pairs $(\mathbf{x}_i, \mathbf{x}_j)$ of points on the attractor, embedded in mth dimensional phase space, whose distance is smaller than ε. The ansatz is then that $C(m, \varepsilon, N)$ behaves like a power law as $N \to \infty, \varepsilon \to 0$. The correlation dimension and entropy are then defined as

$$D_c = \lim_{\varepsilon \to 0} \lim_{m,N \to \infty} \frac{\partial \log C(m, \varepsilon, N)}{\partial \log \varepsilon},$$
$$h_c = \lim_{\varepsilon \to 0} \lim_{m \cdot N \to \infty} \ln \frac{C(m, \varepsilon, N)}{C(m+1, \varepsilon, N)}. \tag{20}$$

Numerical results are given in Fig. 9 and Table 1. The approximations of the correlation sums were done for the use of the TI.SE.AN. package [Hegger *et al.*, 1999; Kantz & Schreiber, 1999] while the algorithm of the Lyapunov exponent spectrum is based on the Oseledets multiplicative ergodic theorem and is an implementation of a robust algorithm from [Choe, 2005]. In Fig. 9(a), we present the Lyapunov exponent spectrum of (F) for $b = 0.5$ and $a \in (1.8, 4.2)$ (compare with Fig. 3). The calculations were done in MAPLE using the algorithms from [Choe, 2005]. In Figs. 9(b) and 9(c) we have outlined with a bold line the range of ε where scaling occurs and is the same for increasing embedding dimensions. A comprehensive analysis of these plots is discussed in [Kantz & Schreiber, 1999].

Table 1. Numerical estimates of the invariant characteristics of the attractors of Fig. 10.

Fig.$1_{(a,b)}$	Lyapynov Spectrum	D_c	h_c
(2.1, 0.5)	(−0.035, 0.000)	1.000	0.000
(3.23, 0.5)	(−0.207, 0.057)	1.162	0.153
(3.4, 0.5)	(−0.043, 0.060)	1.304	0.150
(3.96, 0.5)	(−0.248, 0.099)	1.178	0.220
(2.78, 0.8)	(−0.051, 0.032)	1.326	0.110
(2.8, 0.8)	(−0.011, 0.015)	1.500	0.080
(2.9, 0.8)	(−0.045, 0.038)	1.480	0.012
(6.5, 0.8)	(−0.132, 0.116)	1.470	0.350
(2.5, 1.2)	(−0.025, 0.028)	1.458	0.149
(2.6, 1.2)	(0.004, 0.052)	1.686	0.213

5.4. *Multiscroll attractors*

We conclude this section discussing an interesting concern, posed by one of the reviewers. In view of Fig. $1_{(6.5,0.8)}$ we were kindly asked whether (F) could generate multitori attractors either by controlling one of its parameters or adding some suitable controller. The problem of generating multiscroll chaotic attractors using a chaotic oscillator is most interesting among the nonlinear dynamics and circuit systems community and is mainly focused on continuous time systems (see for example [Yu *et al.*, 2012; Lu *et al.*, 2004] or a thorough tutorial on this problem, the theory and the methods [Lu & Chen, 2006]). We do not know of a study

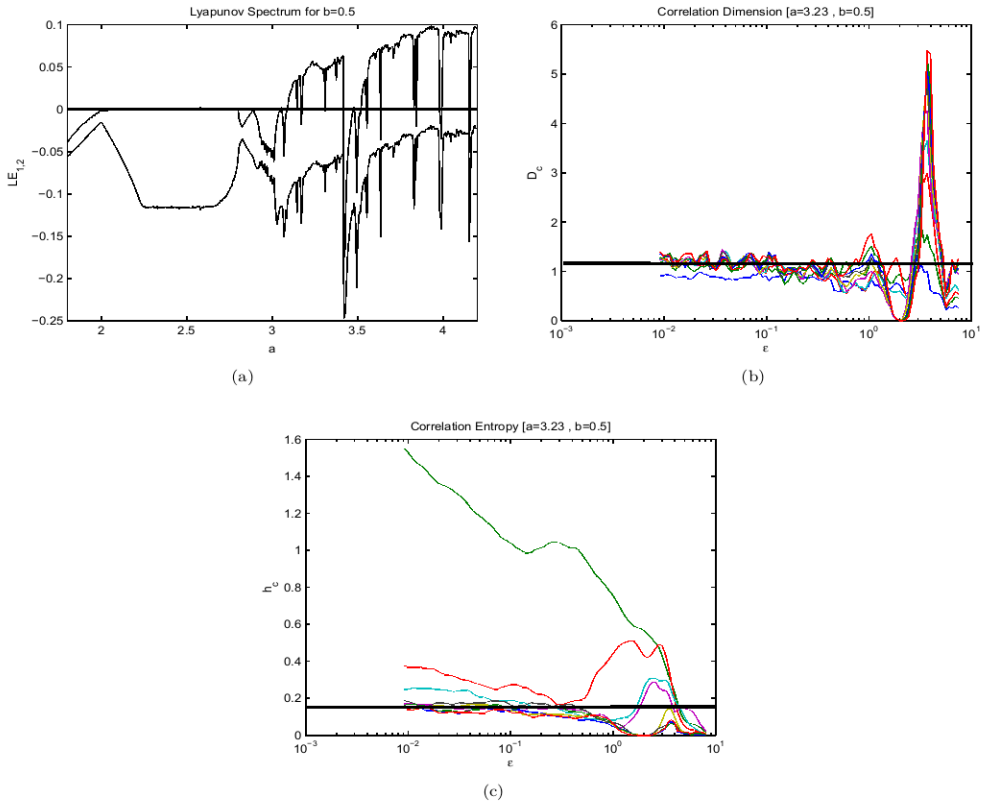

Fig. 9. (a) The Lyapunov exponent spectrum for $b = 0.5$. Compare it with the bifurcation diagram in Fig. 2. (b) The D_c estimator. (c) The h_c estimation.

of this problem exclusively for discrete time systems [Lu & Chen, 2006] that includes a section for digital but discretized systems.

Although a clear multiscroll attractor generation was not identified for (F) by a simple tuning of its parameters, we believe that there are feedback control laws which can generate multiscroll attractors in the broad sense. The key to this problem is for the researcher to come up with a law which will add fixed (or periodic) points which will remain unstable for fixed parameter values. This requirement has a quick response and that is to make the control law, more like a perturbation to (F).

So we respond to the question by the following illustrating example. Consider the controlled system

$$F\begin{pmatrix} x \\ y \end{pmatrix} = \begin{pmatrix} -\dfrac{6.5u(x,y)}{1+y^2} \\ x + 0.8y \end{pmatrix} = \begin{pmatrix} -\dfrac{6.5x}{1+y^2} \\ x + 0.8y \end{pmatrix} + \varepsilon \begin{pmatrix} x^3 \\ 0 \end{pmatrix}. \quad (21)$$

For $\varepsilon = 0$, we get the unperturbed system $F_{6.5,0.8}$ (see Fig. 1). For $\varepsilon > 0$ the additional fixed

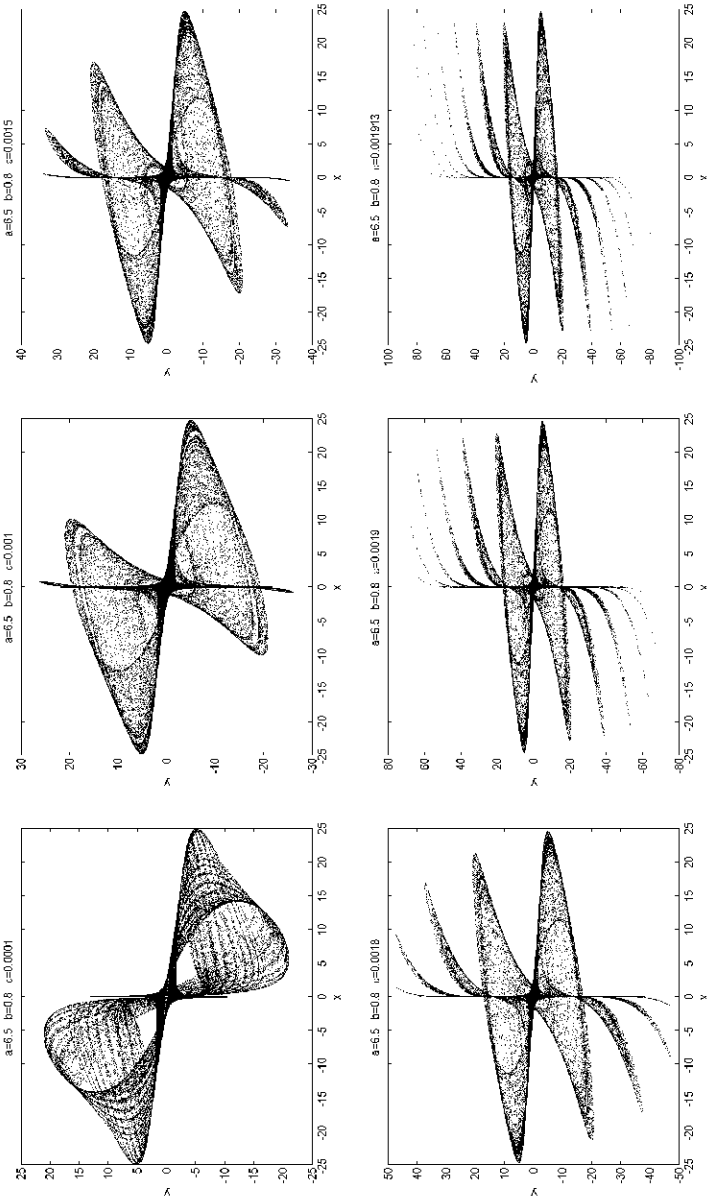

Fig. 10. Phase Plots of the controlled version of (F) for small positive values of ε which generates multiscroll attractors.

points are $\tilde{x} = \pm 0.2\sqrt{\frac{1-4\cdot 10^{-2}\varepsilon+\sqrt{16\cdot 10^{-4}\varepsilon^2+1.12\varepsilon+1}}{8\cdot 10^{-2}\varepsilon}}y$, $\tilde{y} = \pm\sqrt{\frac{1-4\cdot 10^{-2}\varepsilon+\sqrt{16\cdot 10^{-4}\varepsilon^2+1.12\varepsilon+1}}{8\cdot 10^{-2}\varepsilon}}$ and it can be verified that they are saddle points (for example, for $\varepsilon = 0.001$ the eigenvalues of the Jacobian evaluated at $\tilde{x}, \tilde{y}$ are 1.5019 and 0.7997).

The multiscroll behavior is outlined in the phase plots of Fig. 10. Although the proposed nonlinear feedback control law is rather trivial, it illustrates the fact that (F) is capable of generating multiscroll chaos. We conjecture that any law of the form $\varepsilon x^{2N+1}, N \in \mathbb{Z}$ could form an interesting family of multiscroll chaos controls. A systematic study and classification of such laws would be an interesting issue.

6. Discussion and Concluding Remarks

In this work, we have presented and studied the system (F); one of the simplest examples of rational planar maps with very rich nonlinear behavior. For $a > 0$, the system exhibits mainly symmetric attractors which do not merge, as long as $|b| < 1$. For $a > 1$, the origin is a saddle fixed point with y-axis as the global stable manifold to which the attractors approach as a gets larger, yet they never overrun it. A typical orbit will oscillate between the second and third quadrants getting attracted by an anti-symmetric attractor. For $|b| < 1$ all solutions are bounded although it can be verified that as a gets larger and larger the magnitude of the limit set increases.

For a specific range of parameter values, (F) exhibits transition to chaos through either intermittency or period-doubling bifurcations. The quasiperiodic behavior is ubiquitous for numerous values of the parameters, however there is no convincing evidence that (F) goes to chaos via the standard Ruelle–Takens–Newhouse quasiperiodic scenario. There are more to be done however. It should be noted that for the special case $b = 0$, exhaustive numerical inspection has revealed no strange attractors for $a > 0$.

Moreover, the case $b < 0$ reveals more interesting phenomena. In this work, we have argued that (F) is invertible and in a subset of $\mathbb{R}^2$ where a closed form of its inverse was proved.

Furthermore, in [Somarakis & Baras, 2011b] we have discussed the existence of the strange attractors using more rigorous methods. There we applied the method of fixed point index, a computer assisted topological method, introduced in [Zgliczynski, 1997], where we showed that a strange attractor exists for the map $F^{(2)}_{2.5,1.2}$.

There are also other issues that require further numerical investigation such as the type of intermittencies or the phenomenon of hyperchaoticity.

Acknowledgments

This work is supported by the Army Research Office award number W911NF-08-1-0238 to Ohio State University. The authors are also thankful to the anonymous reviewer for most helpful comments, remarks and corrections.

References

Carr, J. [1981] *Application of Centre Manifold Theory*, 1st edition (Springer).

Chang, L. D. [2005] "A new two-dimensional discrete chaotic system with rational fraction and its tracking and synchronization," *Chaos Solit. Fract.* **22**.

Choe, H. G. [2005] *Computational Ergodic Theory*, 1st edition (Springer).

Grassberger, P. & Procaccia, I. [1983] "Measuring the strangeness of strange attractors," *Physica D* **9**, 189.

Guckenheimer, J. & Holmes, P. [2002] *Nonlinear Oscillations, Dynamical Systems and Bifurcations of Vector Fields*, 7th edition (Springer).

Hegger, R., Kantz, H. & Schreiber, T. [1999] "Practical implementation of nonlinear time series methods: The tisean package," *Chaos* **9**, 413.

Kantz, H. & Schreiber, T. [1999] *Nonlinear Time Series Analysis* (Cambridge University Press, UK).

Lu, J. & Chen, G. [2006] "Generating multiscroll chaotic attractors: Theories, methods and applications," *Int. J. Bifurcation and Chaos* **16**, 775–858.

Lu, J., Yu, X., Han, F. & Chen, G. [2004] "Generating 3-d multi-scroll chaotic attractors: A hysteresis series switching method," *Automatica* **40**, 1677–1687.

Lu, L. & Wu, K. [2004] "A new discrete chaotic system with rational fraction and its dynamical behaviors," *Chaos Solit. Fract.* **24**.

Newhouse, S., Ruelle, D. & Takens, F. [1978] "Occurence of strange axiom a attractors near quasi-periodic flows on t^m, $m \geq 3$," *Commun. Math. Phys.*, pp. 35–40.

Ott, E. [2002] *Chaos in Dynamical Systems* (Cambridge University Press).

Pomeau, Y. & Manneville, P. [1980] "Intermittent transition to turbulence in dissipative dynamical systems," *Commun. Math. Phys.* **74**.

Somarakis, C. & Baras, J. S. [2011a] *4th International Chaotic Modeling and Simulation* (Crete, Greece).

Somarakis, C. & Baras, J. S. [2011b] "The dynamics of a simple rational map," Applied Mathematics Technical Report TR 2011-08, Institute For Systems Research.

Wiggins, S. [2003] *Introduction to Applied Nonlinear Dynamical Systems and Chaos*, 2nd edition (Springer).

Yu, S., Lu, J., Yu, X. & Chen, G. [2012] "Design and implementation of grid multiwing hyperchaotic Lorenz system family via switching control and constructing super-heteroclinic loops," *IEEE Trans. Circuits Syst.* **59-I**, 1015–1028.

Zeraoulia, E. & Sprott, J. [2011a] "On the dynamics of a new simple 2-d rational discrete mapping," *Int. J. Bifurcation and Chaos* **21**, 155–160.

Zeraoulia, E. & Sprott, J. [2011b] "Some open problems in chaos theory and dynamics," *Int. J. Open Problems in Computer Science and Mathematics* **4**, 1–9.

Zgliczynski, P. [1997] "Computer assisted proof of the horseshoe dynamics in the Henon map," *Rand. Comput. Dyn.* **5**, 1–17.

Appendix A
Center Manifold Theory

Consider the system

$$\begin{aligned} x_{k+1} &= C_1 x_k + f_1(x_k, y_k) \\ y_{k+1} &= C_2 y_k + f_2(x_k, y_k) \end{aligned} \tag{A.1}$$

where $x \in \mathbb{R}^n$, $y \in \mathbb{R}^m$ and C_1, C_2 are constant matrices of appropriate dimensions such that all the eigenvalues of C_1 are on the unit circle and all those of C_2 within the unit circle. The functions f_1 and f_2 are C^2 with $f_1(0,0) = f_2(0,0) = 0$ and $Df_1(0,0) = Df_2(0,0) = 0$. An invariant manifold for (A.1) $y = h(x)$ where h is smooth, is called *center manifold* if $h(0) = 0, Dh(0) = 0$. If f, g are identically nonzero, then the following theorem holds.

Theorem 1 [Carr, 1981]. *There exists $\delta > 0$ and $h \in C^2$ such that $y = h(x)$ defines a center manifold for (A.1).*

The form of $h(x)$ is of vital importance but it can only be approximated. If we substitute $y_k = h(x_k)$ into the second equation of (A.1) then

$$\begin{aligned} y_{k+1} = h(x_{k+1}) &= h(C_1 x_k + f_1(x_k, y_k)) \\ &= C_2 h(x_k) + f_2(x_k, h(x_k)). \end{aligned} \tag{A.2}$$

The identity in the right part of (A.2) defines the *center manifold equation* and can be utilized assuming that h has a particular polynomial form for solutions close to the equilibrium, say $h(x) = a_0 + a_1 x + a_2 x^2 + a_3 x^3 + O(x^4)$. The flow on the center manifold is governed by the n-dimensional system

$$u_{k+1} = A u_k + f(u_k, h(u_k)). \tag{A.3}$$

It can be shown that (A.2) contains all the necessary information needed to determine the asymptotic behavior of small solutions of (A.3) using (A.2) and (A.1). In our case, the type and behavior of the bifurcations of the initial system are equivalent to the ones of the reduced (A.3) by Theorem 2, p. 4 of [Carr, 1981].

Appendix B
Neimark–Sacker Bifurcations

We state the theorem used to prove the existence of a Neimark–Sacker bifurcation. Consider a map in the following Normal Form [Wiggins, 2003; Guckenheimer & Holmes, 2002]

$$\begin{pmatrix} x \\ y \end{pmatrix} \to D_a \begin{pmatrix} x \\ y \end{pmatrix} + \begin{pmatrix} f(x,y) \\ g(x,y) \end{pmatrix} \tag{B.1}$$

where by D_a we denote a linearized matrix controlled by the critical parameter a. Consider the expressions

$$\begin{aligned} \xi_{20} &= \frac{1}{8}[(f_{xx} - f_{yy} + 2g_{xy}) + i(g_{xx} - g_{yy} - 2f_{xy})] \\ \xi_{11} &= \frac{1}{4}[(f_{xx} + f_{yy}) + i(g_{xx} + g_{yy})] \\ \xi_{02} &= \frac{1}{8}[(f_{xx} - f_{yy} 2g_{xy}) + i(g_{xx} - g_{yy} + 2f_{xy})] \\ \xi_{21} &= \frac{1}{16}[(f_{xxx} - f_{xyy} + g_{xxy} + g_{yyy}) \\ &\quad + i(g_{xxx} - g_{xyy} - f_{xxy} - f_{yyy})]. \end{aligned} \tag{B.2}$$

Theorem 2 [Guckenheimer & Holmes, 2002]. *Let (B.1) be a one-parameter family of mappings which has a smooth family of fixed points $x(a)$ at which the eigenvalues are complex conjugates. Assume that the following expression evaluated at the critical value a_0 and the fixed point $x(a_0)$ hold*

(SH1) $\mathrm{Re}[\lambda(a_0)] = 0 \Rightarrow \lambda(a_0) = e^{ic}$, $|\lambda(a_0)| = 1$, $\lambda^k(a_0) \neq 1$ *for* $k = 1, 2, 3, 4$

(SH2) $\frac{d}{da}|\lambda(a_0)| = d \neq 0$

(SH3) $S = -\mathrm{Re}[\frac{(1-2\lambda)\bar{\lambda}^2}{1-\lambda}\xi_{11}\xi_{20}] - \frac{1}{2}|\xi_{11}|^2 - |\xi_{02}|^2 + \mathrm{Re}[\bar{\lambda}\xi_{21}] \neq 0.$

Then there is a smooth change of coordinates of (B.1) which in polar form yields

$$(r, \theta) \to (r(1 + d(a - a_0) + ar^2), \theta + c + br^2) + h.o.t.$$

Moreover, there is a two-dimensional surface Σ in $\mathbb{R}^2 \times \mathbb{R}$ having quadratic tangency with the plane at $\mathbb{R}^2 \times \{a_0\}$ which is invariant for (B.1). If $\Sigma \cap \mathbb{R}^2 \times \{a\}$ is larger than a point, it is a curve.

The discussion in [Wiggins, 2003, § 21.3] categorizes the stability and type of the Neimark–Sacker bifurcation according to the signs of S, a and d.